GLIA

WILEY

RESEARCH ARTICLE

TREM2 promotes glioma progression and angiogenesis mediated by microglia/brain macrophages

Xuezhen Chen[1] | Yue Zhao[1] | Yimin Huang[2] | Kaichuan Zhu[1] | Fan Zeng[1] | Junyi Zhao[1] | Huaqiu Zhang[2] | Xinzhou Zhu[1] | Helmut Kettenmann[1,3] | Xianyuan Xiang[1]

[1]Shenzhen Key Laboratory of Immunomodulation for Neurological Diseases, Shenzhen Institutes of Advanced Technology, Chinese Academy of Sciences, Shenzhen, China

[2]Department of Neurosurgery, Tongji Hospital of Tongji Medical College of Huazhong University of Science and Technology, Wuhan, China

[3]Max-Delbrück Center for Molecular Medicine, Berlin, Germany

Correspondence

Helmut Kettenmann and Xianyuan Xiang, Shenzhen Key Laboratory of Immunomodulation for Neurological Diseases, Shenzhen Institutes of Advanced Technology, Chinese Academy of Sciences, Shenzhen 518055, China.
Email: kettenmann@siat.ac.cn and xy.xiang@siat.ac.cn

Abstract

Triggering receptor expressed on myeloid cell 2 (TREM2), a myeloid cell-specific signaling molecule, controls essential functions of microglia and impacts on the pathogenesis of Alzheimer's disease and other neurodegenerative disorders. TREM2 is also highly expressed in tumor-associated macrophages in different types of cancer. Here, we studied whether TREM2 influences glioma progression. We found a gender-dependent effect of glioma growth in wild-type (WT) animals injected with GL261-EGFP glioma cells. Most importantly, TREM2 promotes glioma progression in male but not female animals. The accumulation of glioma-associated microglia/macrophages (GAMs) and CD31$^+$ blood vessel density is reduced in male TREM2-deficient mice. A transcriptomic analysis of glioma tissue revealed that TREM2 deficiency suppresses immune-related genes. In an organotypic slice model devoid of functional vascularization and immune components from periphery, the tumor size was not affected by TREM2-deficiency. In human resection samples from glioblastoma, TREM2 is upregulated in GAMs. Based on the Cancer Genome Atlas Program (TCGA) and the Chinese Glioma Genome Atlas (CGGA) databases, the TREM2 expression levels were negatively correlated with survival. Thus, the TREM2-dependent crosstalk between GAMs and the vasculature formation promotes glioma growth.

KEYWORDS

angiogenesis, brain tumor, glioma, macrophage, microglia, microglial cells, TREM2

1 | INTRODUCTION

Glioma is the most common form of tumor within the central nervous system (CNS), and is classified into low-grade (II) and high-grade (III or IV) glioblastomas (GBM) (Gutmann & Kettenmann, 2019). GBM is the most lethal malignant brain tumor in adults; currently, no effective treatment is available. The incidence of GBM is higher in men than women, with a ratio of 1.6:1 (Davis, 2016; Ostrom, Rubin et al., 2018). With the standard treatments, namely surgical resection followed by radio−/chemotherapy, the median survival rates for GBM patients remain disappointedly low with a 5-year survival rate of 9.8% (Schaff & Mellinghoff, 2023), although

Xuezhen Chen and Yue Zhao contribute equally as first authors.

Helmut Kettenmann and Xianyuan Xiang contribute equally as corresponding authors.

the standard therapy is more effective in female than in male patients (Yang et al., 2019). Immunotherapy with checkpoint inhibitors has shown great success in various solid tumors, whereas less than 10% of GBM patients show long-term responses (Jackson et al., 2019). The complexity and heterogeneity of the brain tumor microenvironment (TME) is one of the main obstacles for developing novel therapeutic strategies (Dumas et al., 2020). In addition to cancer cells, TME contains various non-cancerous cell types, including immune and endothelial cells (Wu et al., 2021). The communication and reciprocal connections among these cells create an immuno-suppressive environment and actively contribute to GBM progression (Charles et al., 2012; Gutmann & Kettenmann, 2019; Hambardzumyan et al., 2016; Liu et al., 2022).

The majority of immune cells in the GBM environment is represented by the myeloid cell population, composed of brain resident microglia and monocyte-derived macrophages, termed glioma-associated microglia/macrophages (GAMs). They often comprise up to 30%–50% of the tumor mass (Gutmann & Kettenmann, 2019) and outnumber infiltrating T cells (Lim et al., 2018), providing an immunosuppressive and pro-tumorigenic environment. The glioma environment convert GAMs into tumor-promoting cells, which enhances glioma cell proliferation, degrades the extracellular matrix, promotes angiogenesis, and induces T-cell apoptosis (Gutmann & Kettenmann, 2019; Roesch et al., 2018). Therefore, GAMs have become attractive novel targets for glioma therapy. However, the targeting of GAMs using colony-stimulating factor-1 receptor (CSF-1R) inhibitors failed to improve the clinical outcome (Butowski et al., 2016). Consequently, more precise GAMs-regulating targets should be identified to better understand the complex interaction of glioma and glioma associated cells including the vascular system.

Triggering receptor expressed on myeloid cells 2 (TREM2) is exclusively expressed in the myeloid cell lineage, regulating important myeloid cell functions, including proliferation (Schlepckow et al., 2020), migration (Mazaheri et al., 2017), and phagocytosis (Hsieh et al., 2009; Kleinberger et al., 2014; Xiang et al., 2016). TREM2 restrains cytokine production in macrophages in response to LPS stimulation (Turnbull et al., 2006). TREM2 is upregulated in macrophages associated with human and mouse tumors. In a sarcoma mouse model, the inhibition of TREM2 signaling restricts tumor growth and sensitizes the response to anti-PD1 immunotherapy (Katzenelenbogen et al., 2020; Molgora et al., 2020). A humanized antibody targeting TREM2 was currently tested in phase I clinical trials for solid tumors (Binnewies et al., 2021). While there is good evidence for the involvement of TREM2 in other solid tumors, its role in glioma remains to be determined.

In this study, we used the orthotopic GL261 mouse glioma model (Haddad et al., 2021) in vivo and the well-established organotypic brain slice (OBS) glioma model (Hu et al., 2015; Huang et al., 2020) ex vivo to explore the functional role of TREM2 in the context of GBM progression. We found that glioma volume is reduced in TREM2 deficient male but not in female mice injected with GL261-EGFP. In addition, the density of GAMs and CD31^{+} blood vessels are reduced within the glioma in TREM2-deficient male mice. We conclude that the crosstalk between GAMs and the vasculature mediated by TREM2 has an impact on glioma progression.

2 | METHODS AND MATERIALS

2.1 | Animals

The TREM2 KO (Turnbull et al., 2006) line was kindly provided by Dr. Marco Colonna at the Washington University School of Medicine, St. Louis. The line is maintained at heterozygous breeding and WT or TREM2 KO littermates were used from the offspring. All experiments were approved by the Shenzhen Institute of Advanced Technology, Chinese Academy of Sciences Research Committee, and all experimental procedures involving animals were carried out in strict accordance with the Research Committee's animal user guidelines. Food and water were provided ad libitum. Male and female mice (10–12 weeks) were used in this study.

2.2 | Cell culture

The murine glioma cell line GL261 (American Type Culture Collection) was cultured in Dulbecco's Modified Eagle Medium (DMEM) supplemented with 10% fetal bovine serum (FBS) (Lonsera), 50 units/mL penicillin–streptomycin, and 200 mM glutamine (Invitrogen). GL261 were transduced with lentivirus expressing enhanced green fluorescent protein (EGFP). For primary microglia cultures, Postnatal day 1 (P1) –P3 mice were used. After the extraction of the brains, meninges and cerebellum were removed and brains were put on ice with Hanks balanced salt solution (HBSS, Beyotime Biotechnology), subsequently minced into small pieces before adding trypsin (10 mg/mL, Beyotime Biotechnology) and DNase (0.5 mg/mL, Beyotime Biotechnology) in PBS. After 2–3 min of incubation, the reaction was blocked by adding DMEM containing 10% FBS. After removal of the medium, 10 U of DNase was added and the cells were mechanically dissociated. The dissociated cell suspension was centrifuged for 10 min at 300g at 4°C. The pellet was resuspended in DMEM supplements (10% heat-inactivated FBS, Lonsera), 50 units/mL penicillin–streptomycin, and 200 mM glutamine (Invitrogen) and was plated (cells from 2 brains/flask) in poly-L-lysine-coated T75 flasks (Corning). A complete change of medium was performed 24 h after plating to remove excess debris. Thereafter, half of the medium was changed every 2 days. After 9–10 days in culture, primary microglia were collected from the supernatant and were plated at a density of 3×10^5 in one well of a 12-well plate. The supernatant of the cultivated primary microglia was collected 3 days after plating. The microglia conditioned medium was stored at −20°C until further usage.

Bone marrow derived macrophages (BMDM) were prepared as previously described (Xiang et al., 2018). Briefly, the bone marrow cells were flushed out using advanced RPMI 1640 (Life Technologies). Cells were differentiated using culture medium [advanced RPMI 1640 supplemented with 2 mM L-Glutamine, 10% FBS, 100 U/mL penicillin,

100 μg/mL streptomycin) supplemented with 50 ng/mL murine M-CSF (R&D System) for 7 days in non-cell culture treated dishes. The mature BMDM were scraped and replated onto 12 well plates in a density of 300,000 cells/well, and culture medium was supplement with 10 ng/mL murine M-CSF. BMDM conditional medium were collected 3 days after plating and stored at −20°C until further usage.

2.3 | In vivo glioma model

Ten- to twelve-week-old WT and TREM2 KO mice were used for the in vivo studies to investigate glioma progression. Mice were anesthetized, immobilized, and mounted onto a stereotactic frame in the flat-skull position (Digital Stereotaxic Instruments, 68018 RWD Life Science). After skin incision, the skull was carefully drilled at the point located at 1 mm anterior and 1.8 mm lateral to the bregma with Hamilton tip. A 2 μL syringe with a blunt tip (Mikroliterspritze 7001N, Hamilton) was inserted to a depth of 4.5 mm and retracted to a depth of 4 mm from the skull into the right caudate putamen. Then, 0.5 μL of a cell suspension containing 1×10^4 GL261-EGFP glioma cells were slowly injected into the brain within 2.5 min. The needle was then slowly retracted from the injection canal, and the skin was sutured with a surgical sewing cone (RWD Life Science). After surgery, the mice were kept on a 37°C heated pat until awake. Mice were monitored daily and perfused with paraformaldehyde (PFA) 21 days after injection, and brain samples were collected for the immunohistochemistry and RNA sequencing.

2.4 | Tumor size measurements

After animal perfusion, brains were fixed with 4% PFA in PBS (Beyotime Biotechnology) overnight at 4°C and dehydrated with 30% sucrose for 48 h at 4°C. To prepare brain sections, we cut brains into 40 μm sections, collected every 12th slice, and mounted it on a glass slide. Other slices were put in cryoprotectant solution for immunofluorescence staining and inspection. The EGFP fluorescence signal of the GL261 glioma cells was excited at a wavelength 488 nm and visualized at of 507 nm analyzed by a Zeiss LSM apotome microscope (Carl Zeiss) with a 10 × objective. The glioma area in individual slices was determined based on the fluorescence area analyzed with ImageJ software. Tumor volumes were determined by EGFP immunostaining every 12th slice according to the Cavalieri principle (Hu et al., 2015; Huang et al., 2020).

2.5 | Mice survival assay

For survival analysis, an independent cohort of mice was used. The GL261-EGFP-injected mice were monitored daily from 21 days on until the terminal endpoint. The disease progression was scored from 0 to 20 based on the severity of following criteria: loss of body weight, hunchback, low reaction to stimulation, tarnished fur, or movement problem (normal = 0, slight burden = 5, medium burden = 10, severe burden = 20). When the sum of scores of these criteria is equal or larger than 20, the animals were sacrificed.

2.6 | Organotypic brain slice cultures

Organotypic brain slice (OBS) were prepared as described previously (Huang et al., 2020) with minor modifications. P5-8 WT and TREM2 KO mice were sacrificed, brains were taken out, and placed in cold HBSS (Beyotime Biotechnology). The left and right hemispheres were separated and cut coronally into 250 μm thick slices using McIlwain tissue chopper (Ted Pella Inc.) under a laminar hood. Six to eight slices were transferred individually into a Millicell Cell Culture Insert, 30 mm, hydrophilic polytetrafluoroethylene polymer, 0.4 μm (PICM0RG50 Millipore) in 6-well plate with culture medium containing 50% DMEM, 25% Basal Medium Eagle (BME), 25% heat inactivated horse serum, 10 mM HEPES, 10 mM tris, 0.1% glucose, 2 nM glutamax, NaOH PH7.4, and insulin 5 μg/mL (Invitrogen). Culture medium was changed every 2 days. After 5 days of culture maintenance, 5000 GL261-EGFP cells in a volume of 0.1 μL were inoculated into the brain slices using a 1 μL syringe (Hamilton). The medium was changed and collected every 2 days. Six days after GL261-EGFP inoculation, the slices were washed three times with PBS and fixed with 4% PFA at room temperature for 20 min. Samples were washed with PBS and kept in 4°C until further processing.

2.7 | CCK-8 kit assay

A total of 5000 GL261-EGFP cells per well were seeded in a 96-well plate. Sixteen hours after plating, medium was changed to DMEM only or DMEM mixed with WT primary microglia conditional medium in a one-to-one ratio or DMEM mixed with KO primary microglia conditional medium in a one to one ratio. The culture was kept in a 37°C incubator for 48 h. The CCK-8 reagent (Beyotime Biotechnology) was added (10 μL per well) and incubated for 2 h. Plates were measured with a multireader at 450 nm absorbance. Results were normalized to the absorbance of the control group DMEM only. BMDM conditioned medium was similarly tested.

2.8 | Genotyping

Littermate controls were used in all experiments. For genotyping, genomic DNA was purified from tail biopsies by isopropanol precipitation, and the TREM2 locus harboring the knock-out mutation was amplified by polymerase chain reaction (PCR) using forward primer1 5′-CCCTAGGAATTCCTGGATTCTCCC-3′, forward primer2 5′-TTAC-ACAAGACTGGAGCCCTGAGGA-3′ and reverse primer 5′-TCTGAC-CACAGGTGTTCCCG-3′. PCR products were subsequently analyzed by 2% PCR agarose gel electrophoresis. The band of wild type was

detected at 231 bp and deletion in homozygous was detected at 316 bp.

2.9 | Immunofluorescence staining and image processing

Twenty-one days post-injection, mice brains were harvested and perfused with PBS followed by 4% PFA solution (Beyotime Biotechnology); 40 μm free-floating tissue sections were prepared as described above. Slices were washed three times with PBS for 5 min and blocked with 5% of donkey serum or 5% of goat serum in PBS with 0.5% Triton-X (93443, Sigma). Primary antibodies were added overnight at 1:100 for CD31 (AF3628, R&D Systems), 1:500 dilution for Iba1 (ab5076, Abcam or 019-19741, Wako), 1:400 for Ki67 (9129, Cell Signaling Technology), 1:500 for CD 8 (ab217344, Abcam) at 4°C. Iba1 and CD31 were detected using the secondary antibody Cy3-conjugated donkey anti-goat IgG (1:500, Beyotime), while CD8 and Ki67 were detected by Alexa-647-conjugated donkey anti-rabbit secondary antibody (1:500, Thermofisher). All brain slices were stained with DAPI (Beyotime) to detect the nuclei, and then were mounted in Aqua-Poly/Mount (Polysciences). Fluorescence images were taken with the apotome microscope or confocal microscope (Carl Zeiss) through Z-stack scanning under 20 × objective or 40 × objective, and the whole brain images were taken with TissueFAXS Q + Systems (TissueGnostics) with 20 × objective. Then, 2–3 sections per biological replicate were analyzed and quantified for each mouse model, and the number of biological replicates per mouse model is indicated in the figure legends.

2.10 | Immunohistochemistry of human tissue material

Immunofluorescent staining was performed in human glioma tissues. The present study was approved by the Tongji Hospital Committee for human studies (process number: TJ-IRB20211162). Primary antibodies included Iba1 (1:500, Abcam), Trem2 (1:400, Cell Signaling Technology) and CD31 (1:800, Cell Signaling Technology). Briefly, tumor sections were deparaffinized, rehydrated, and antigen-retrieved by standard procedures. Then, samples were blocked with a PBS solution containing 1% BSA plus 0.3% Triton X-100 for 2 h at room temperature and then incubated with indicated primary antibody overnight at 4°C followed by the fluorescence-conjugated second antibody (1:100, Proteintech, cat: SA00013-6, SA00009-2, and SA00013-1) at room temperature for 2 h. After being counterstained with DAPI for 5 min, sections were mounted on glass and subjected to microscopy. The images were acquired with a fluorescence microscope (Olympus, CKX53).

2.11 | RNA sequencing

GBM tissue and tools were pre-chilled with liquid nitrogen and the tissue was grinded into powder. A portion of the powder was transferred to TRIzol (Sigma) lysis buffer. RNA was extracted using a standard protocol (Guneykaya et al., 2018). Briefly, TRIzol lysis were mixed with 300 μL chloroform/isoamyl alcohol (24:1) and 2/3 volume of isopropyl alcohol was added. It was centrifuged at 17,500 × g for 25 min at 4°C. The supernatant was discarded, and the precipitation subsequently washed with 0.9 mL 75% ethanol and dissolved in 20 μL DEPC-H_2O or RNase-free water. RNA quality was controlled using Agilent rna 6000 nano kit (5067-1511, Agilent) according to the manufacturer's instructions. RNA was reverse-transcribed into a cDNA library. Single-stranded circle DNA molecules were replicated via rolling cycle amplification, and a DNA nanoball (DNB), which contained multiple copies of DNA, was generated. Sufficient quality DNBs were then loaded into patterned nanoarrays using high-intensity DNA nanochip technique and sequenced through combinatorial probe-anchor synthesis (cPAS).

2.12 | Statistical analysis

The results are presented as mean ± standard mean error. Differences between the groups were evaluated for significance by two-tailed Student's test (two groups) or two-way analysis of variance (ANOVA) test (more than two groups) using GraphPad Prism 7 (GraphPad Software). Probability (p) values ≤ .05 were considered statistically significant.

3 | RESULTS

3.1 | The tumor volume is reduced in TREM2-deficient GL261 glioma male mice

To study the impact of TREM2 expression on glioma growth, we employed an in vivo mouse experimental glioma model. We injected GL261 mouse glioma cells expressing the fluorescent marker EGFP into the striatum of wild-type (WT) or TREM2 homozygous knock-out (KO) animals. Twenty-one days after tumor inoculation, mice were sacrificed and analyzed for tumor volume size and cellular parameters. Male and female animals were separately analyzed due to the fact that glioblastoma is more frequent in men than in women in a 1.6:1 ratio (Davis, 2016; Ostrom, Rubin et al., 2018). The tumor was visible from the surface of the cortex (Figure 1a). The volume of the tumor was 4.7-fold larger in WT male than in WT female animals (47.86 ± 9.76 vs. 10. 27 ± 2.22 mm³, p = .0001; Figure 1b,c). However, the expression of TREM2 is similar in both genders (Figure S1). In the female group, TREM2 deficiency did not show a significant impact on tumor size (WT 10.27 ± 2.22 vs. KO 10. 07 ± 2.84 mm³; Figure 1b,c). In contrast, in the male animals, the tumor volume was significantly smaller in KO animals compared to the WT counterparts (WT 47.86 ± 9.76 vs. KO 16.73 ± 4.72 mm³, p = .0018; Figure 1b,c). Interestingly, tumor volume in TREM2-deficient male
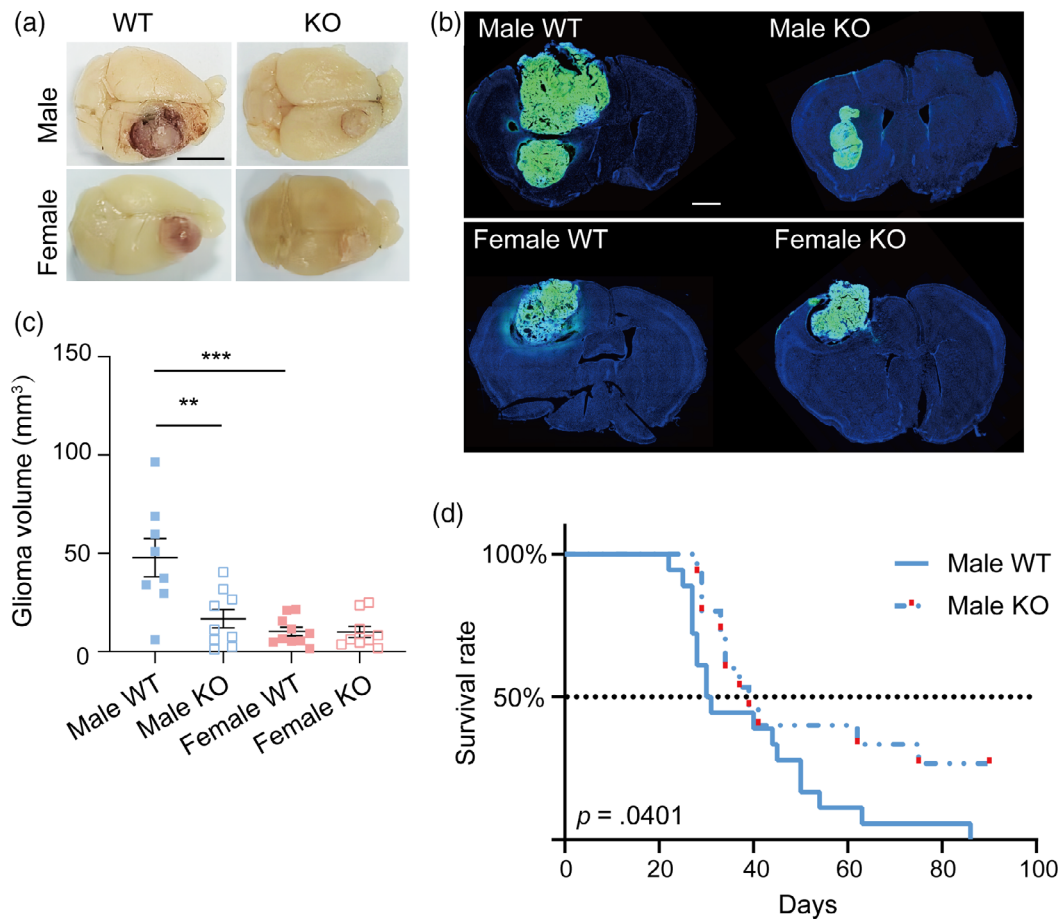
FIGURE 1 The tumor volume is reduced in TREM2-deficient GL261 glioma male mice. (a) Representative images of whole brains with tumors of male and female WT and TREM2 KO mice. Scale bar denotes 1 cm. (b) Representative immunofluorescence images of WT and TREM2 KO coronal brain sections 21 days after stereotactic injection of GL261-EGFP into male and female mice. GL261-EGFP (green); DAPI (blue) (Scale bar, 1 mm). (c) Quantification of glioma volume based on the EGFP signal. Female WT (n = 10), Female KO (n = 9); Male WT (n = 8), Male KO (n = 9); Data are presented as means ± SEM. One-way ANOVA with Bonferroni corrected multiple comparisons. **$p \leq .01$; ***$p \leq .001$. (d) Kaplan–Meier curves represent the cumulative survival of male WT and TREM2 KO mice injected with GL261-EGFP cells (n = 15–18 per group, Log-rank test $p = .0401$).

animals shows no differences compared to female WT or female KO animals, suggesting that the gender effects for GBM could potentially be attributed to TREM2 expression. Collectively, these findings suggest that the GL261 GBM mouse model recapitulates the gender preference, most importantly TREM2 expression promotes tumor progression in male animals. Therefore, we used only the male GL261 GBM mouse model for the subsequent analysis of the mechanistic impact of TREM2 expression on glioma progression.

We further tested the impact of TREM2 on the survival time of tumor-inoculated male mice. Mice were scored daily after 21 days for the following symptoms: body weight, hunchback, low reaction to stimulation, tarnished fur, or movement problems. Animals were sacrificed if they show severe symptoms in the criteria mentioned above. The difference on survival probability between these two genotypes was significantly different when 90 days were assigned as observation endpoint (median survival: WT 30 days vs KO 39 days, $p = .0401$; Figure 1d).

3.2 | TREM2 deficiency results in lower GAMs density at the tumor core and rim in male glioma animals

Since TREM2 is expressed by microglia as well as by monocyte-derived macrophages, we determined the distribution of GAMs in different regions of the GL261-EGFP inoculated male animals. We determined the density of GAMs at the core of the tumor, at the outer rim of the tumor, in the area of adjacent brain tissue denoted as interface (0–0.3 mm away from the EGFP positive cells). Moreover, we analyzed the density in four regions with increasing distance (in 0.3 mm steps) from the tumor (adjacent brain region ABR 1, 0.3–0.6 mm; ABR 2, 0.6–0.9 mm; ABR 3, 0.9–1.2 mm; ABR 4, 1.2–1.5 mm; Figure 2a–c) and at the contralateral side of tumor inoculated hemisphere. In the core of the tumor, the coverage of the Iba1-fluorescent area is significantly higher in WT compared to TREM2 KO animals (12.46% ± 1.27% vs. 6.91 ± 1.00, $p = .0002$; Figure 2b,d). Similarly, WT animals also show higher Iba1-fluorescent
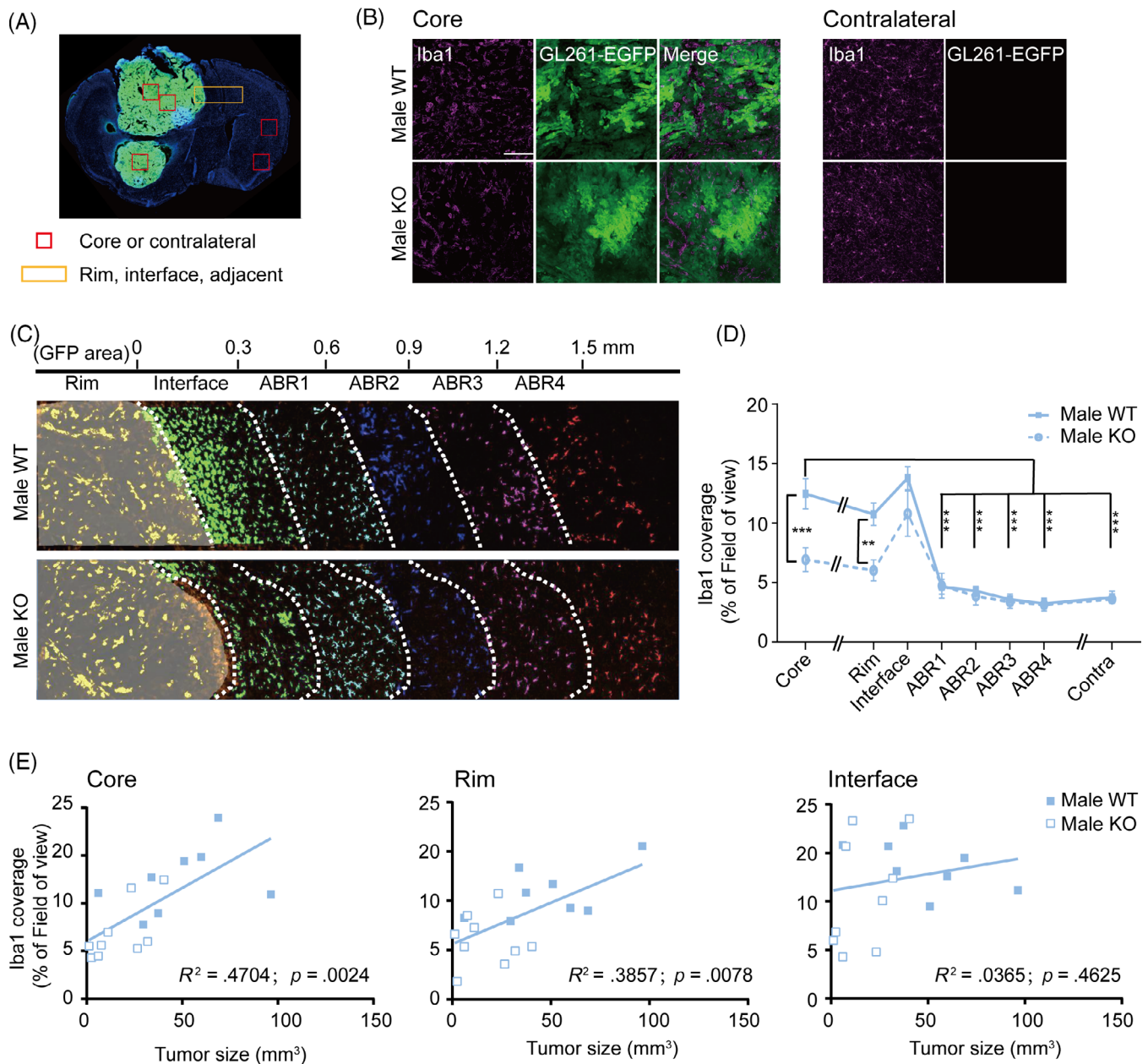
FIGURE 2 TREM2 deficiency results in lower GAMs density at the tumor core and rim in male glioma animals. (a) Overview image showing the regions analyzed for coverage of microglia/macrophages in a tumor bearing male mouse brain. The core region of glioma and contralateral region were chosen with a 0.5×0.5 mm box and the rim region was chosen with 0.5×2.5 mm box. (b) Representative images of Iba1$^+$ cells in the glioma core and contralateral hemisphere from WT (top) and TREM2 KO (bottom) male mice. Iba1 (magenta), GL261-EGFP (green), and merged image. Scale bar denotes 100 μm. (c) Representative immunofluorescence images for microglia/macrophages (Iba1), glioma cells (GL261-EGFP) and merged image of WT and TREM2 KO mice at the rim of glioma including glioma area (up to 0 mm), glioma interface (0–0.3 mm) and adjacent brain region (0.3–1.5 mm). Different color codes for Iba1$^+$ cells in different subdivided regions. (d) Quantification of the percentage of the Iba1 coverage in the analyzed regions as described in C (WT $n = 8$, KO $n = 9$). Data are presented as means ± SEM. $^*p \leq .05$, $^{**}p \leq .01$, two-way ANOVA with Bonferroni corrected multiple comparisons. (e) Correlation between Iba1 coverage and glioma size in the core (left), rim (middle) and the interface (right) as defined in (c).

area at the rim of tumor (10.75% ± 0.95%, vs. 6.02 ± 0.88, $p = .0024$; Figure 2c,d). However, the Iba1-fluorescent area is not significantly different between the two genotypes in the tumor-brain interface, the ABR1-4 (Figure 2c,d), and the contralateral area (Figure 2b,d). Notably, the distribution of GAMs at the tumor-brain interface is denser compared to the rim of the tumor (Figure 2c,d), similar to the data that have

been reported in patient glioblastoma tissue (Yin et al., 2022), indicating that the GL261 glioblastoma mouse model represents the clinical features of GAMs distribution.

We also tested the correlation between the density of GAMs and glioma volume in these male animals. GAMs density is positively correlated with glioma volume in the core and rim region of glioma

(Figure 2e left and middle panel). However, there is no positive correlation between the glioma volume and the density of GAMs in the interface region (Figure 2e right panel). These data suggest that the density of GAMs within the glioma correlates with glioma size. More importantly, these data suggest the reduced GAMs density in the core and rim of tumor in the TREM2 KO animals correlates with a smaller tumor size.

To further characterize the immune environment of the glioma tissue, we analyzed the density of CD8$^+$ T cells within the tumor. The density of CD8$^+$ T cell population is not influenced by the TREM2 expression (Figure S2a,b).

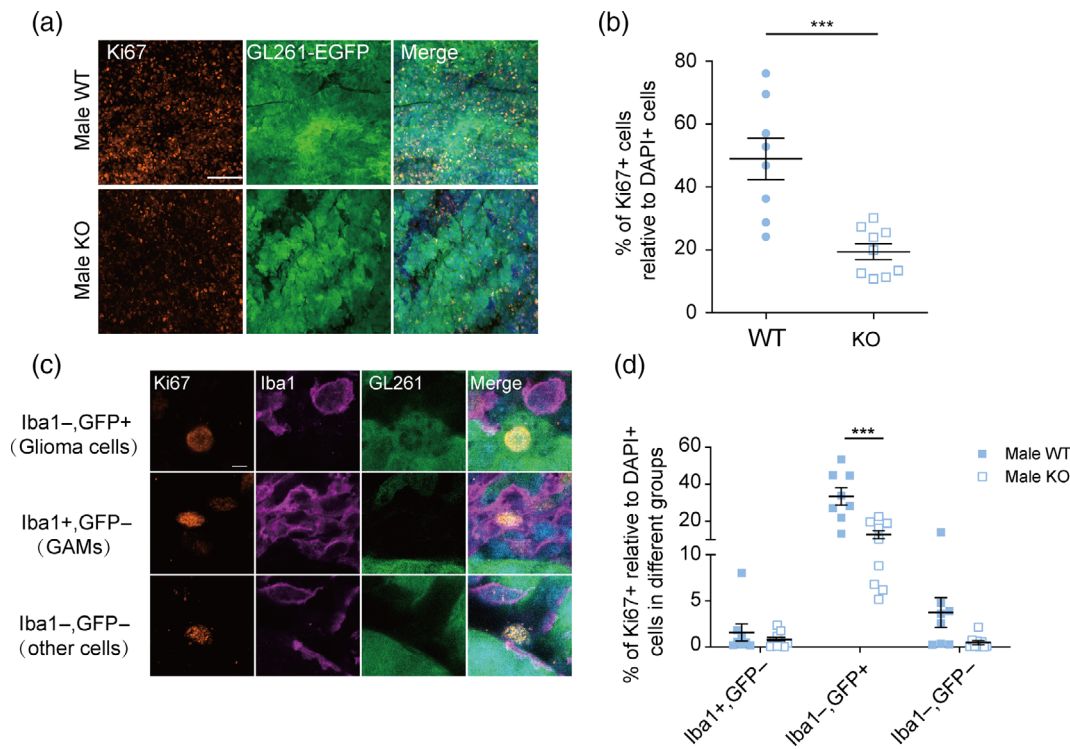## 3.3 | TREM2 deficiency leads to a lower proliferation rate in glioma cells, but not in GAMs

We next attempted to study the proliferation of glioma cells, GAMs, and remaining cell types in the tumor environment determined by Ki67 immunofluorescence staining. These experiments were performed in male mice only. The Ki67 signal was co-localized with DAPI. The Ki67$^+$ cell number was normalized to total DAPI$^+$ cell number in a given region. We found that the percentage of Ki67 positive cells is lower in TREM2 KO GBM as compared to WT (Figure 3a,b).

We further divided the Ki67$^+$ cells into three categories, namely in Iba1$^-$/EGFP$^+$ (glioma cells), Iba1$^+$/EGFP$^-$ (GAMs), and Iba1$^-$/EGFP$^-$ (other brain cells) (Figure 3c,d). In the GL261 tumor cell population, Ki67 is significantly higher in WT animals compared to TREM2 KO animals, indicating that the proliferation rate of tumor cells is reduced due to the loss of TREM2 (Figure 3c,d). In the GAMs population, the Ki67$^+$ population is not significantly different in WT versus KO animals (Figure 3c,d), suggesting that TREM2 deficiency did not show a significant impact on the proliferation rate of GAMs. Similarly, we found no significant difference in Ki67$^+$ cells in WT and KO animals in the population of Iba1$^-$/EGFP$^-$ (other brain cells; Figure 3c,d).

3.4 | The density of CD31$^+$ blood vessels in the glioma is reduced in the TREM2-deficient mice

Since angiogenesis is an important factor in malignant gliomas influencing tumor growth and progression (Fischer et al., 2005), we quantified the density of CD31$^+$ blood vessels in the tumor core, the tumor rim and adjacent brain regions, similar to the analysis for Iba1 coverage as described above (Figure 2a). As expected, the density of blood vessels (CD31$^+$ coverage) is increased in the core, rim and tumor-brain interface region as compared to the contralateral side in


FIGURE 3 TREM2 deficiency leads to a lower proliferation rate in glioma cells but not in GAMs. (a) Images of Ki67 staining (left), EGFP fluorescence of GL261 glioma cells (middle) and merged image (right) for WT (top) and TREM2 KO mice (bottom). The bar denotes 100 μm. (b) Quantification of the percentage of Ki67$^+$ cells among the DAPI$^+$ cells in the glioma tissue of WT and TREM2 KO male mice. (c) Corresponding images of Ki67, Iba1, EGFP (from GL261-EGFP cells) and merged labeling showing examples of Ki67 cells co-labeled with glioma cells (top, Iba1$-$, EGFP$+$), GAMs (middle, Iba1$+$, EGFP$-$) and other cells (lower, Iba1$-$, EGFP$-$) in glioma. The bar denotes 5 μm. (d) Quantification of the images shown in (c). Data are presented as means ± SEM. Two-way ANOVA with Bonferroni corrected multiple comparisons. ***$p \le .001$.

both genotypes, indicating a strong angiogenesis in the tumor-related environment (Figure 4a–c). The density of CD31$^+$ blood vessels in the areas further away from tumor (0.3–1.5 mm, defined as ABR1-4 similar as described above for GAMs density analysis) is not significantly different compared to the contralateral site in both genotype (Figure 4b,c). These results indicate that the increase in vessel density is restricted to the glioma tissue and its closely adjacent region (designated as interface). Importantly, in the glioma core, rim and the

tumor-brain interface region, the coverage of CD31$^+$ regions is higher in WT compared to TREM2 KO animals (Core: WT 9.159% ± 1.216% vs. KO 5.272 ± 1.246, $p = .0033$; Rim: WT 11.878% ± 1.430% vs. KO 5.277 ± 1.075, $p < .0001$; Interface: WT 6.629% ± 1.461% vs. KO 4.043 ± 0.808%, $p = .048$; Figure 4a–c). Next, we analyzed the vessel length in the core region. The CD31$^+$ vessel length in the core region is significantly longer in the WT compared TREM2 KO animals (Figure 4d). The glioma size is positively correlated with
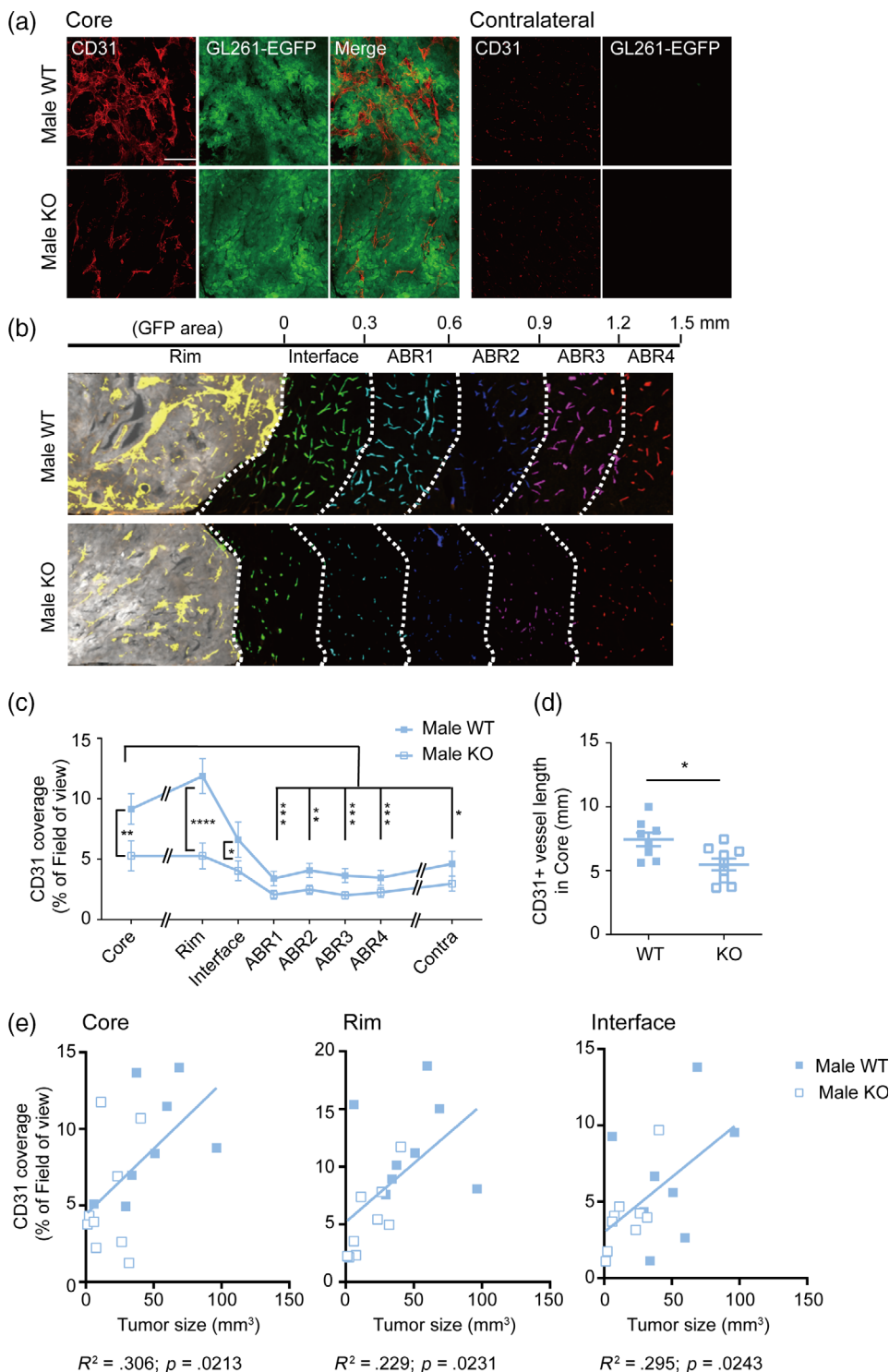
FIGURE 4 The density of CD31$^+$ blood vessels in the glioma tissue is reduced in TREM2-deficient mice. (a) Representative images of vessels in the core of the glioma and contralateral site of WT (top image) and TREM2 KO (bottom image) male mice. Immunofluorescence staining for CD31 (magenta), EGFP (for GL261-EGFP cells) (green) and a merged image. Scale bar denotes 100 μm. (b) Representative images for vessels (CD31$^+$) of WT and TREM2 KO animals at the rim and interface of glioma. Different color codes for vessels in different sub divided regions as described in detail in the legend to Figure 2. (c) Quantification of the percentage of CD31$^+$ immunofluorescence coverage in the regions as defined in (b). (WT $n = 8$, KO $n = 9$) Data are presented as means ± SEM. *$p \le .05$; **$p \le .01$; ***$p \le .001$; ****$p \le .0001$, two-way ANOVA with Bonferroni corrected multiple comparisons. (d) Quantification of vessel length based on CD31 staining in the glioma core of WT and TREM2 KO. (e) Correlation between CD31 coverage and glioma size in the core (left), rim (middle) and the interface (right) as defined in the legend to Figure 2.
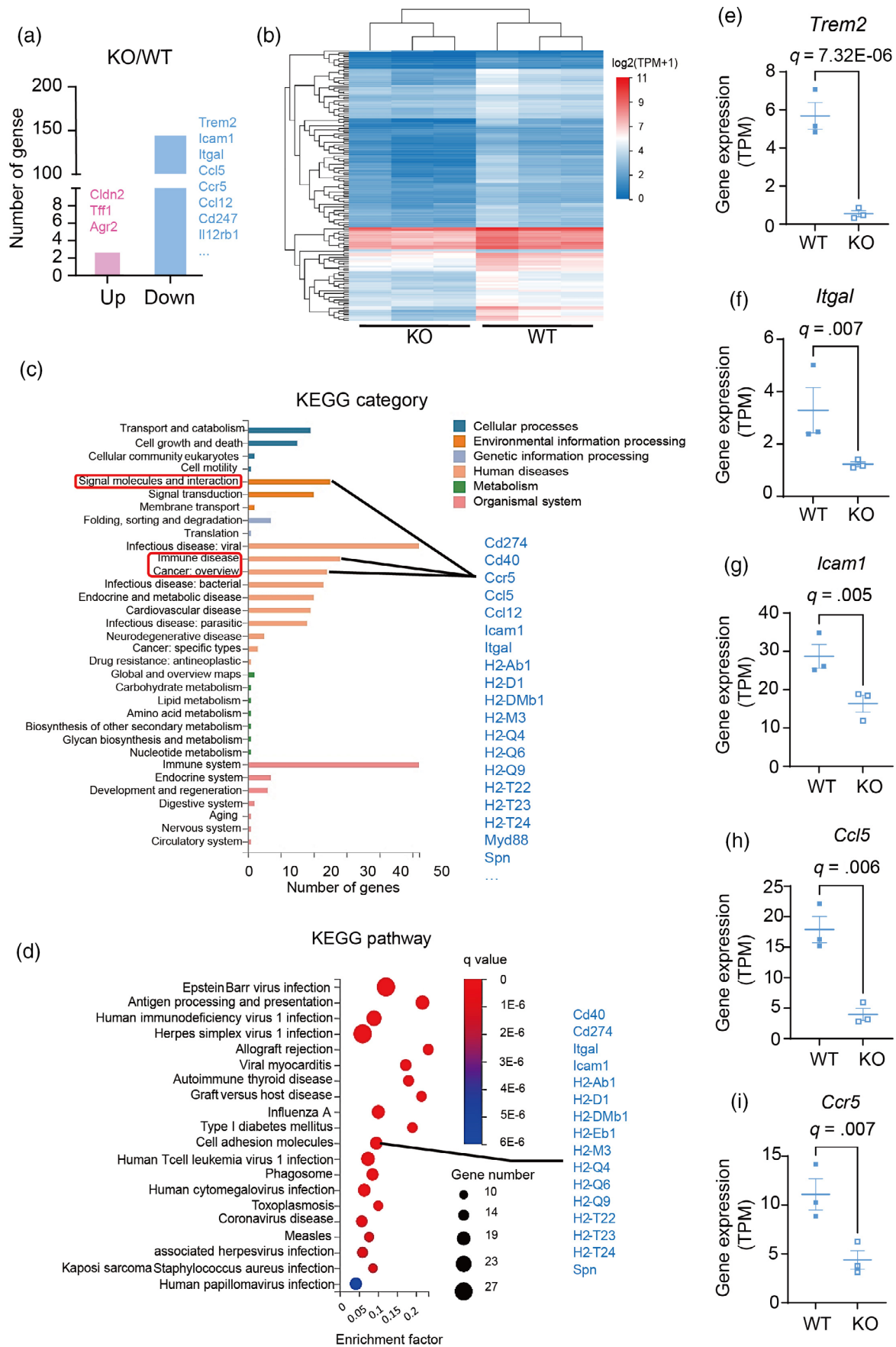
CD31$^+$ area in core, rim and interface regions, respectively (Figure 4e), suggesting a positive role of vascularization on tumor growth. These data suggest that the TREM2 deficiency attenuates angiogenesis in the glioma tissue.

3.5 | TREM2 deficiency suppresses immune-related genes

To understand the underlying mechanisms how TREM2 deficiency leads to reduced vasculature, we performed a transcriptomic analysis of the glioma tissue. Twenty-one days after GL261-EGFP inoculation, the glioma tissue was dissected from WT or TREM2 KO male mice for RNA extraction and bulk RNA-seq. A similar number of genes was detected in both genotypes (16,353 ± 207 in WT vs. 16,208 ± 23 in KO). At the settings of log$_2$|FC| ≥ 1 and adjusted p ≤ .05, 144 downregulated and 3 upregulated genes were discovered (Figure 5a and Figure S3a). Samples from WT and TREM2 KO animals show a clear separated cluster, and 144 out of 147 differentially expressed genes (DEGs) are downregulated in TREM2 KO samples (Figure 5a,b and Figure S3b). KEGG pathway analysis was carried out to identify involved signaling pathways for TREM2 functions in glioma pathology (Figure 5c). KEGG category analysis showed that a large proportion of DEGs were immune genes which may participate in immune diseases (28 genes), cancers (24 genes) and, signaling molecules and interaction (25 genes, signaling molecules and receptors; Figure 5c). Interestingly, we noticed that a group of cell adhesion molecules in KEGG pathway analysis were downregulated in KO glioma, including 11 major histocompatibility complex (MHC) I and MHC II cluster genes (MHC I cluster: H2-D1, H2-M3, H2-Q4, H2-Q6, H2-Q9, H2-T22, H2-T23, H2-T24; MHC II cluster: H2-Ab1, H2-DMb1, H2-Eb1; Figure 5c,d). The reduction of MHC gene cluster may suggest a reduced antigen presentation in GBM from KO animals compared to WT and may contribute to immune escape and impaired functions of CD4$^+$/CD8$^+$ cells and NK cells in GBM (Burster et al., 2021; Kilian et al., 2023).

Some immune signaling genes which can modulate angiogenesis were also identified in the downregulated group (KEGG pathway category: signaling molecules and interaction; Figure 5c), including two cell adhesion molecules Icam1 (Lim et al., 2022) and Itgal (Silva et al., 2008; Zhang, Wang et al., 2022), chemokines Ccl12 and Ccl5 (Suffee et al., 2011; Wang et al., 2015), the chemokine receptor Ccr5 and inflammatory signaling adaptor Myd88 (Zhang et al., 2020). Based on the adjusted p value (q value), these genes are downregulated in GBM from TREM2 KO animals (Figure 5e–i and Figure S3c,d). In contrast, one of the three upregulated genes in KO animals

(Figure 5a and Figure S3e), Tff1 (Shi et al., 2019; Zhang, Zhang et al., 2022), inhibits angiogenesis in cancer progression, which support the notion that TREM2 positively regulates angiogenesis in glioma environment. We checked the expression of the well-known angiogenic factor VEGFA (Machein & Plate, 2000; Osterberg et al., 2016) in the RNAseq dataset, as well as by measuring the total amount of VEGFA in GBM lysate. No differences were found in the RNA and protein levels of VEGFA in GBM tissue between the two genotypes (Figure S3f,g).

In addition, we examined whether TREM2 is correlated with these angiogenic related immune genes in glioma patients. In datasets from Chinese Glioma Genome Atlas (CGGA) (Zhao et al., 2021) RNA-seq dataset, TREM2 expression was found to be positively correlated with Itgal, Icam1, Ccl5, Ccr5, and Myd88 expressions in glioma patients (Figure S4a–e). Tff1 expression can only be found in one of the three microarray datasets and was negatively correlated to TREM2 expression in recurrent glioma patients (Figure S4f).

In summary, the transcriptomic analysis revealed that TREM2 depletion on one hand inhibits genes in MHC I and II clusters, which may suppress antigen presentation; on the other hand, TREM2 depletion suppresses immune genes that show pro-angiogenic functions.

3.6 | TREM2 shows no impact on glioma growth in isolated ex vivo and in vitro systems

To study if a functional vasculature system is a prerequisite for TREM2-mediated impact on glioma size, we analyzed glioma growth in the organotypic brain slice glioma model (OBS), where the tissue contains all the major brain cells including microglia, but lacks a functional vasculature system and an influence on the peripheral immune system including the immigration of blood monocytes. Slices were prepared from postnatal day 5–8 WT or TREM2 KO animals, cultivated for 5 days and subsequently injected with 5000 GL261-EGFP cells (Figure 6a). Six days after glioma cell inoculation, the volume occupied by EGFP-labeled glioma cells was determined by immunohistochemistry and confocal microscopy with z stack images. The volume of glioma is not significantly different between WT and KO, indicating that TREM2 has no effect on glioma growth in the isolated ex vivo model (Figure 6b,c). In addition, no difference was found regarding the density of Iba1$^+$ cells in the glioma area of WT and KO OBS tissue (Figure 6d,e). TREM2 is expressed by Iba1$^+$ microglia, as shown by colocalization of TREM2 and Iba1 in the WT OBS (Figure 6d), and the specificity of the immunostaining is shown by lack of TREM2 signal in the KO tissue (Figure 6d). After normalized to Iba1$^+$ area, TREM2 coverage is higher within glioma compared

FIGURE 5 TREM2 deficiency suppresses immune-related genes. (a) The number of differentially expressed genes (DEGs) in the GBM sample in TREM2 KO mice compared to WT mice. Also, 144 downregulated (some examples are indicated) and three upregulated genes were identified. (b) Heat map of log2 transcripts per kilobase million +1 [log (TPM + 1)] of 147 DEGs from WT and TREM2 KO samples with adjusted p ≤ .05 and log$_2$|FC| ≥ 1. (c, d) KEGG category (c: genes listed on the right refers to the categories as indicated) and pathway (d) analysis of DEGs: the genes listed at the right refer to genes in Cell adhesion molecules pathway. (e–i) Gene expression (TPM) of *Trem2l), Itgal* (f), *Icam1* (g), *Ccl5* (h) and *Ccr5* (i) (n = 3). q values (adjusted p value) are indicated.
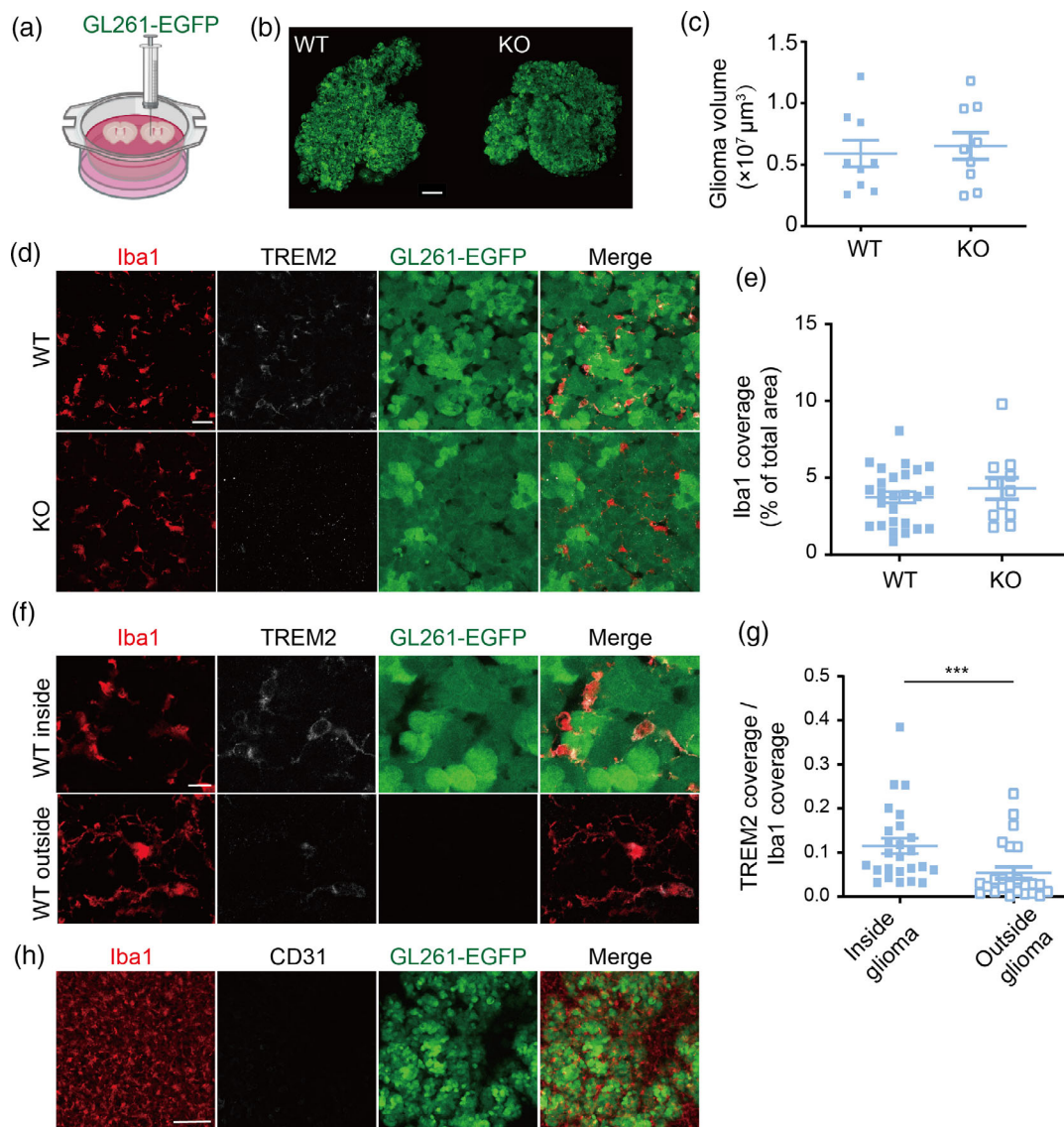
FIGURE 6 TREM2 show no impact on glioma growth in isolated ex vivo system. (a) Schematic view of the organotypic brain slice culture (OBS) inoculated with GL261-EGFP glioma cells. (b) Representative immunofluorescence images of glioma (green) in WT and TREM2 KO OBS (Scale bar, 200 μm). (c) Quantification of glioma volume based on the EGFP signal. (d) Representative image for Iba1 (red), TREM2 (white), GL261-EGFP (green) and merge image of WT (top) and TREM2 KO (bottom) from OBS glioma model (Scale bar, 20 μm). (e) Quantification of the percentage of Iba1$^+$ covered area in the glioma region (GL261-EGFP). (f) Representative image for Iba1 (red), TREM2 (white), GL261-EGFP (green) and merged image of a region inside (top) and outside (bottom) of the glioma in a slice from a WT animal (Scale bar, 10 μm). (g) Quantification of the percentage of TREM2$^+$ covered area (normalized to Iba1$^+$ area) inside and outside of glioma. (h) Representative immunofluorescence image of Iba1 (red) and CD31 (white) and EGFP (green) within the glioma region in WT and TREM2 KO OBS (Scale bar, 100 μm). Data are presented as means ± SEM. ***$p \leq .001$, student t-test.

to tumor free tissue (Figure 6f,g), suggesting that glioma inoculation stimulates TREM2 expression in WT OBS. As expected, no CD31$^+$ vessel can be detected within the glioma area in this ex vivo model (Figure 6h).

To further validate if TREM2 deficiency in microglia would have a direct impact on glioma cell proliferation, we incubated GL261 cells with conditional medium from WT or TREM2 KO primary microglia, followed by Cell Counting Kit-8 (CCK-8) assay to quantify cell density and viability. In line with previous reports (Huang et al., 2020),

microglia conditioned medium strongly stimulated the proliferation of GL261 cells resulting in higher viability as compared to unstimulated cells (Figure S5a). However, we found no difference of viable glioma cell numbers when stimulated with either WT or TREM2 KO microglia-produced conditioned medium (Figure S5a), supporting the view that TREM2 deficient microglia do not affect glioma growth via soluble factors. Of note, conditional medium from both WT and TREM2 KO bone marrow derived macrophages (BMDM) shows no impact on GL261 proliferation in this in vitro assay (Figure S5b).

3.7 | TREM2 is upregulated in GAMs in human glioma tissue and negatively correlates with patient survival

To evaluate the TREM2 expression level in the human glioma environment, we immunostained human brain sections from 11 GBM and two epilepsy patients for TREM2 and Iba1, as a marker for GAMs. The TREM2 level is higher in GBM cases compared to epilepsy tissue (Figure 7a,b). Most importantly, most of the TREM2 positive signal is co-localized with Iba1 in the GBM cases (Figure 7a,b), suggesting TREM2 is expressed by GAMs in the tumor environment.

To confirm the evaluated TREM2 expression in the human glioma environment, we first performed a systematic meta-analysis on The Cancer Genome Atlas Program (TCGA) GBM-Agilent 4502A (Figure 7c), TCGA GBM-HG-U133A (Figure 7d), TCGA GBM-RNA-seq (Figure 7e), TCGA GBMLGG RNA-seq (Figure 7f), CGGA (Figure 7g) database utilizing the bioinformatics platform GlioVis (http://gliovis.bioinfo.cnio.es/; Bowman et al., 2017). The expression of TREM2 is higher in GBM compared to nontumor samples in all datasets (Figure 7c–e). Moreover, TREM2 expression is higher in GBM compared to other types of glioma in both TCGA GBMLGG and CGGA datasets (Figure 7f,g). TREM2 is expressed by cells from the myeloid lineage, including microglia, macrophages, and dendritic cells (Colonna, 2003; Xiang et al., 2016). To further study the expression pattern of TREM2 in GBM, we analyzed the Brain Tumor Immune Micro Environment dataset (https://joycelab.shinyapps.io/braintime/; Klemm et al., 2020). The expression of TREM2 is significantly higher in microglia and monocyte derived-macrophages (MDM) compared to CD45$^-$ cells, and this enrichment of TREM2 in microglia and MDM is regardless of the isocitrate dehydrogenase (IDH) genetic status (Figure 7h). Our immunohistochemistry analysis of tissue from GBM patients is in line with these datasets, suggesting that TREM2 is highly expressed by GAMs in the GBM environment.

To assess the correlation of TREM2 expression and the probability of survival in glioma patients, we again used the GlioVis data portal for analysis (Bowman et al., 2017). In two different datasets, TCGA HG-U133A and TCGA Agilent 4502A, patients with higher TREM2 expression show significantly lower survival probability (Figure 7i), indicating high TREM2 expression is detrimental for glioma patients, which is similar to what we detected in the GL261 mouse glioma model.

4 | DISCUSSION

In many neurodegenerative disorders, including Alzheimer's disease (Lewcock et al., 2020; Schlepckow et al., 2020; Wang et al., 2020), amyotrophic lateral sclerosis (Xie et al., 2022), and frontotemporal dementia (Kleinberger et al., 2017), TREM2 has a beneficial role. In contrast, in the MCA/1956 sarcoma model, TREM2 has a detrimental role on tumor growth by modulating the immune landscape (Katzenelenbogen et al., 2020; Molgora et al., 2020). Although it has been shown that TREM2 is highly expressed in the glioma

environment (Molgora et al., 2020), the functional role of TREM2 in glioma is largely unknown. In the current study, we used the GL261 glioma mouse model to show that TREM2 deficiency leads to a reduced glioma size, results in less accumulation of GAMs in the glioma tissue and an attenuated vessel growth. TREM2 acts in a gender-specific fashion in that these TREM2-dependent changes were only observed in male, but not in female animals. This uncovered a previously unknown gender-dependent feature of TREM2 function.

The incidence of glioma in males and females is about 1.6–1 (Ho et al., 2014; Ostrom, Gittleman et al., 2018). Moreover, female glioma patients have a longer survival time than male (Ostrom, Rubin et al., 2018). This evidence suggests that both the incidence and glioma progression is influenced by gender. It has even been suggested that therapeutic strategies should be optimized depending on treatment in a gender-specific manner (Massey et al., 2021). Moreover, our data indicate that the male mice had a larger tumor volume compared to female mice, suggesting that this model can be exploited to study the gender impact on glioma growth. Of note, the gender difference on glioma progression is likely TREM2-independent since the expression level of TREM2 in GBM tissue is similar between two genders. Thus, we postulate that TREM2 in combination with unknow gender-dependent factors influences GBM growth by altering the immune microenvironment and vasculature system.

In the last years, it has become apparent that microglia from male and female mice are quite distinct (VanRyzin et al., 2018, 2020). Microglia in male and female mice differ in structure, function, and transcriptomic and proteomic profiles. Male microglia are more frequent in specific brain areas, have a higher antigen-presenting capacity, and appear to have a higher potential to respond to stimuli such as ATP (Guneykaya et al., 2018). Gender-specific differences in microglial functions and features must not necessarily be due to intrinsic genetic differences but could also be influenced by extrinsic gender-specific cues. Deletion of neuroligin-4, a protein expressed by neurons and not by microglia, is linked to autism spectrum disorders and has a gender-specific impact on microglia. Male microglia show a lower cell density, a less ramified morphology, a reduced response to injury and purinergic signaling specifically in the hippocampal CA3 region (Guneykaya et al., 2023).

An important issue is how a microglia-specific gene deletion, namely of TREM2, affects glioma growth and angiogenesis in combination with a lower number of GAMs in the tumor. What are the pathways of that interaction? In our in vitro studies we applied supernatant from WT and TREM2 KO microglia to glioma cells and determined glioma cells number. While we confirmed former studies that the microglia supernatant increased glioma cell number, there was no significant difference between WT and TREM2 KO. This implies that soluble factors derived from microglia cannot explain the effect of TREM2 KO on glioma growth (with all the cautions relying on an in vitro model). We cannot exclude that physical contact might be a factor but it is more likely that the glioma cell growth is indirectly affected by the TREM2 deletion.

Blood vessels in the tumor are larger and more frequent than in the normal tissue with irregular lumen diameters, they are dilated and
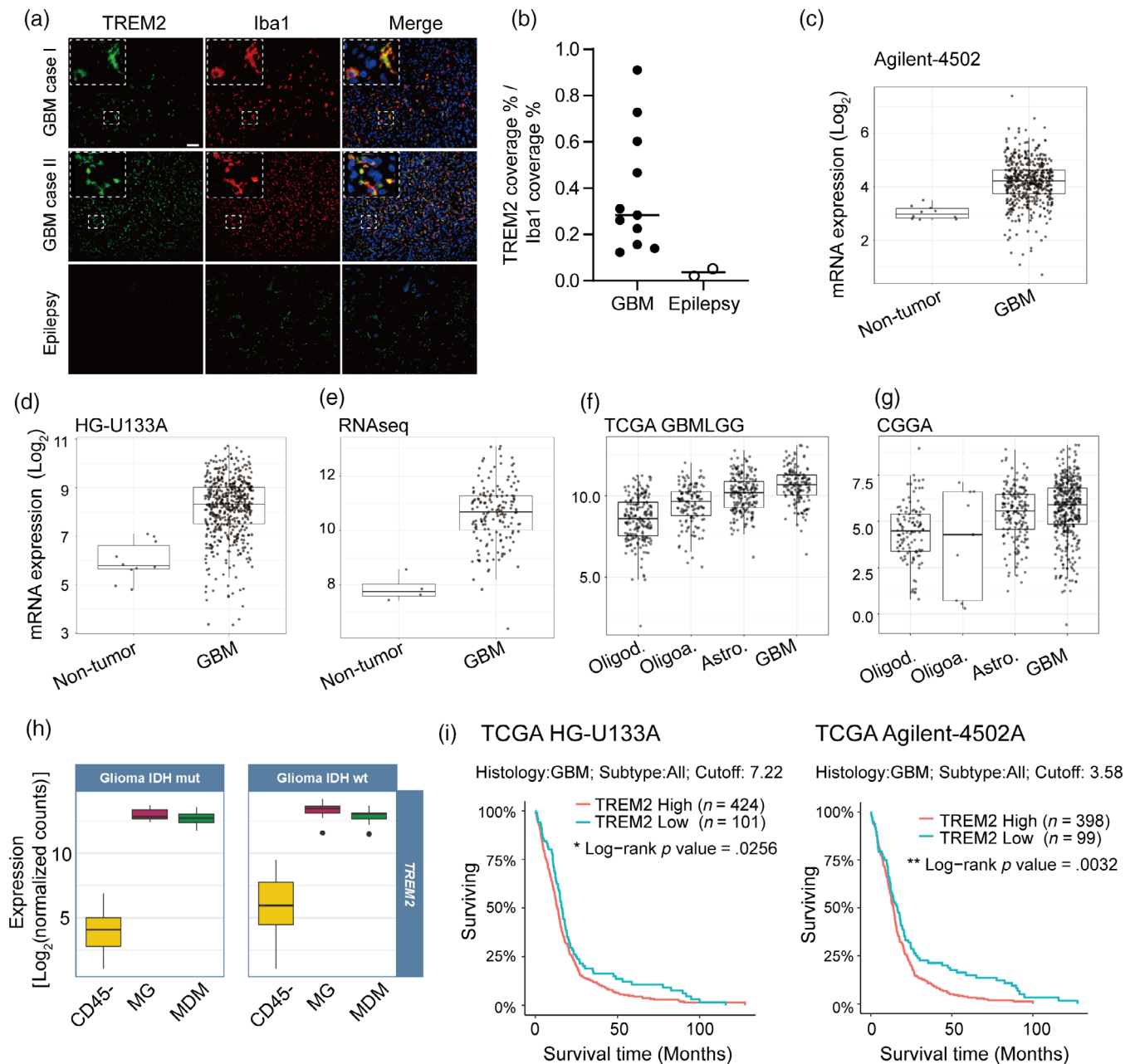
FIGURE 7 TREM2 is upregulated in GAMs in human glioma tissue and negatively correlates with patient survival. (a) Representative images of TREM2 (green), Iba1 (red) and merged images from two GBM patient samples (top and middle) and epilepsy (bottom) tissue from a patient. The insets at the top left are four times enlarged images of the region delineated by the square in the center of the image (Scale bar, 50 μm). (b) Corresponding quantification of TREM2$^+$ area (normalized to Iba1$^+$ area) from 11 GBM samples and two epilepsy samples. (c–g) TREM2 mRNA expression level from different datasets: TCGA-Agilent-4502 (c), TCGA-Hu-U133A (d), TCGA-RNAI (e), TCGA-GBMLGG (f), CGGA (g). In (c–e) GBM tissue is compared to non-tumor tissue, while in (e, f) oligodendro-glioma, oligo-astrocytoma, astrocytoma and GBM cases are compared. (h) TREM2 mRNA expression level in different cell types (CD45-negative cells, MG, microglia; MDM, monocyte derived macrophages) based on the Brain Tumor Immune Micro Environment database distinguishing GBM with IDH mutations and IDH wildtype. (i) Survival probabilities of patients with high and low TREM2 expression level. Optimal cutoff method from the bioinformatic platform GlioVis (http://gliovis.bioinfo.cnio.es/) was used and the cutoff value are indicated in figure. Left: dataset from TCGA HG-U133A; Right: dataset from TCGA Agilent-4502A.

highly permeable, and branch irregularly (De Bock et al., 2011). Angiogenesis is essential for tumor growth and progression (De Bock et al., 2011). As expected, we found that the vessel density is significantly higher within the glioma as well as in the glioma brain interface region. More importantly, the tumor size is positively correlated with vessel density in the glioma region. We found that the density of CD31$^+$ vessels is significantly higher in glioma region from WT animals compared to TREM2 KO. This could lead to the hypothesis

that microglial TREM2 indirectly promotes glioma progression via enhancing the angiogenesis in the glioma environment. We also found that the total vessel length is longer in the core region of glioma from WT animal compared to KO. Interestingly, TREM2 deletion shows no impact on glioma size in the isolated OBS glioma model where no functional vasculature system is present, arguing a TREM2-dependent angiogenic effect could promote glioma progression. It should, in addition, be noted that the OBS glioma does not only lack a functional vasculature system, but also lacks the immigrating cells from the blood system such as monocytes. Both features could play a role.

One possibility is that GAMs promote angiogenesis in a TREM2 controlled fashion. Indeed pro-angiogenic molecules are highly expressed by GAMs (Brandenburg et al., 2016). Our RNAseq analysis revealed that TREM2 deficiency suppresses the expression of several immune genes related with angiogenesis, including _Ccl5_, _Ccr5_, _Ccl12_, _Icam1_, and _Itgal_. In the similar vein, these angiogenesis related immune genes are positively correlated with TREM2 expression in CGGA datasets. These TREM2-dependent factors may promote vascularization within tumor environment, which would explain our finding that tumors in WT animals are larger as compared to TREM2 KO. Itgal is a stromal regulator of murine low-grade glioma growth, and it also regulates Ccl5 production (De Andrade Costa et al., 2022). The Ccl5-Ccr5 signaling pathway promotes VEGF-dependent angiogenesis in the osteosarcoma xenograft animal model (Wang et al., 2015). Although, _vegfa_ is reduced in a TREM2-deficient AD model (Griciuc et al., 2019), its expression is similar when comparing WT and TREM2 KO GBM model. It is possible that the reduced Ccl5-Ccr5 signaling diminished the VEGFA-mediated angiogenic effects. VEGF is an important factor in tumor vascularization but it has a suppressive effect on the immunologic and proangiogenic function of microglia/macrophages in a glioblastoma rodent model (Turkowski et al., 2018). A very interesting candidate is the CXCL2-CXCR2 signaling pathway. In isolated microglia/macrophages from glioma, CXCL2 was strongly up-regulated and showed a higher angiogenic activity than VEGF. Blocking the CXCL2-CXCR2 signaling pathway resulted in considerably diminished glioma sizes (Brandenburg et al., 2016).

In addition to the potential pro-angiogenic role, these factors might also directly stimulate glioma growth. For example, the CCL5-CCR5 axis mediates activation of Akt, and subsequently induces proliferation and invasive behavior of glioma cells (Zhao et al., 2015). Knockdown of Ccl5 promotes glioma cell survival in vitro, and increases the survival in a glioblastoma mouse model (Pan et al., 2017).

We also found a lower density of GAMs in the glioma environment in TREM2 KO animals as compared to WT. Since the number of Ki67$^+$ GAMs is similar between these two genotypes, it is likely that TREM2 deficiency impairs the recruitment of monocytes rather than the proliferation of intrinsic microglia. This would be consistent with our observation that the density of Iba1$^+$ is similar in WT OBS glioma model compared to TREM2 KO, where the contribution of peripheral monocytes is lacking.

In summary, our study reveals a gender-specific pro-tumorigenic function of TREM2 in glioma. It is due to a complex interplay between GAMs which expresses our gene of interest, namely TREM2, and the glioma cells and its vasculature and potentially the invading immune cells. Further studies should address the detailed molecular mechanism of TREM2-dependent angiogenesis in glioma. Coincidentally, a recently published study shows that TREM2-deficiency decreases tumor growth and increased survival in the SB28 glioma model suggesting that TREM2 inhibition can be a potential therapeutic strategy for GBM patients, however, no gender dimorphism was shown (Sun et al., 2023). Thus, TREM2 inhibition has emerged as a novel therapeutic strategy for glioma suppression.

AUTHOR CONTRIBUTIONS

ACKNOWLEDGMENTS

FUNDING INFORMATION

CONFLICT OF INTEREST STATEMENT

No competing interests are declared.

DATA AVAILABILITY STATEMENT

All data supporting the findings from this study are available from the authors upon reasonable request.

ORCID

Helmut Kettenmann https://orcid.org/0000-0001-8208-0291
Xianyuan Xiang https://orcid.org/0000-0002-8125-9027

REFERENCES

Binnewies, M., Pollack, J. L., Rudolph, J., Dash, S., Abushawish, M., Lee, T., Jahchan, N. S., Canaday, P., Lu, E., Norng, M., Mankikar, S., Liu, V. M., Du, X., Chen, A., Mehta, R., Palmer, R., Juric, V., Liang, L., Baker, K. P., …

Sriram, V. (2021). Targeting TREM2 on tumor-associated macrophages enhances immunotherapy. *Cell Reports*, *37*, 109844. https://doi.org/10.1016/j.celrep.2021.109844

Bowman, R. L., Wang, Q., Carro, A., Verhaak, R. G. W., & Squatrito, M. (2017). GlioVis data portal for visualization and analysis of brain tumor expression datasets. *Neuro-Oncology*, *19*, 139–141.

Brandenburg, S., Müller, A., Turkowski, K., Radev, Y. T., Rot, S., Schmidt, C., Bungert, A. D., Acker, G., Schorr, A., Hippe, A., Miller, K., Heppner, F. L., Homey, B., & Vajkoczy, P. (2016). Resident microglia rather than peripheral macrophages promote vascularization in brain tumors and are source of alternative pro-angiogenic factors. *Acta Neuropathologica*, *131*, 365–378.

Burster, T., Gärtner, F., Bulach, C., Zhanapiya, A., Gihring, A., & Knippschild, U. (2021). Regulation of MHC I molecules in glioblastoma cells and the sensitizing of NK cells. *Pharmaceuticals (Basel)*, *14*, 1–15.

Butowski, N., Colman, H., De Groot, J. F., Omuro, A. M., Nayak, L., Wen, P. Y., Cloughesy, T. F., Marimuthu, A., Haidar, S., Perry, A., Huse, J., Phillips, J., West, B. L., Nolop, K. B., Hsu, H. H., Ligon, K. L., Molinaro, A. M., & Prados, M. (2016). Orally administered colony stimulating factor 1 receptor inhibitor PLX3397 in recurrent glioblastoma: An Ivy Foundation Early Phase Clinical Trials Consortium phase II study. *Neuro-Oncology*, *18*, 557–564.

Charles, N. A., Holland, E. C., Gilbertson, R., Glass, R., & Kettenmann, H. (2012). The brain tumor microenvironment. *Glia*, *60*, 502–514.

Colonna, M. (2003). Trems in the immune system and beyond. *Nature Reviews Immunology*, *3*, 445–453.

Davis, M. E. (2016). Glioblastoma: Overview of disease and treatment. *Clinical Journal of Oncology Nursing*, *20*, 1–8.

De Andrade Costa, A., Chatterjee, J., Cobb, O., Sanapala, S., Scheaffer, S., Guo, X., Dahiya, S., & Gutmann, D. H. (2022). RNA sequence analysis reveals ITGAL/CD11A as a stromal regulator of murine low-grade glioma growth. *Neuro-Oncology*, *24*, 14–26.

De Bock, K., Cauwenberghs, S., & Carmeliet, P. (2011). Vessel abnormalization: Another hallmark of cancer? Molecular mechanisms and therapeutic implications. *Current Opinion in Genetics & Development*, *21*, 73–79. https://doi.org/10.1016/j.gde.2010.10.008

Dumas, A. A., Pomella, N., Rosser, G., Guglielmi, L., Vinel, C., Millner, T. O., Rees, J., Aley, N., Sheer, D., Wei, J., Marisetty, A., Heimberger, A. B., Bowman, R. L., Brandner, S., Joyce, J. A., & Marino, S. (2020). Microglia promote glioblastoma via mTOR-mediated immunosuppression of the tumour microenvironment. *EMBO Journal*, *39*, e103790.

Fischer, I., Gagner, J. P., Law, M., Newcomb, E. W., & Zagzag, D. (2005). Angiogenesis in gliomas: Biology and molecular pathophysiology. *Brain Pathology*, *15*, 297–310.

Griciuc, A., Patel, S., Federico, A. N., Choi, S. H., Innes, B. J., Oram, M. K., Cereghetti, G., McGinty, D., Anselmo, A., Sadreyev, R. I., Hickman, S. E., El Khoury, J., Colonna, M., & Tanzi, R. E. (2019). TREM2 acts downstream of CD33 in modulating microglial pathology in Alzheimer's disease. *Neuron*, *103*, 820–835.e7. https://doi.org/10.1016/j.neuron.2019.06.010

Guneykaya, D., Ivanov, A., Hernandez, D. P., Haage, V., Wojtas, B., Meyer, N., Maricos, M., Jordan, P., Buonfiglioli, A., Gielniewski, B., Ochocka, N., Cömert, C., Friedrich, C., Artiles, L. S., Kaminska, B., Mertins, P., Beule, D., Kettenmann, H., & Wolf, S. A. (2018). Transcriptional and translational differences of microglia from male and female brains. *Cell Reports*, *24*, 2773–2783.e6.

Guneykaya, D., Ugursu, B., Logiacco, F., Popp, O., Feiks, M. A., Meyer, N., Wendt, S., Semtner, M., Cherif, F., Gauthier, C., Madore, C., Yin, Z., Çınar, Ö., Arslan, T., Gerevich, Z., Mertins, P., Butovsky, O., Kettenmann, H., & Wolf, S. A. (2023). Sex-specific microglia state in the Neuroligin-4 knock-out mouse model of autism spectrum disorder. *Brain, Behavior, and Immunity*, *111*, 61–75.

Gutmann, D. H., & Kettenmann, H. (2019). Microglia/brain macrophages as central drivers of brain tumor pathobiology. *Neuron*, *104*, 442–449. https://doi.org/10.1016/j.neuron.2019.08.028

Haddad, A. F., Young, J. S., Amara, D., Berger, M. S., Raleigh, D. R., Aghi, M. K., & Butowski, N. A. (2021). Mouse models of glioblastoma for the evaluation of novel therapeutic strategies. *Neuro-Oncology Advances*, *3*, vdab100.

Hambardzumyan, D., Gutmann, D. H., & Kettenmann, H. (2016). The role of microglia and macrophages in glioma maintenance and progression. *Nature Neuroscience*, *19*, 20–27.

Ho, V. K. Y., Reijneveld, J. C., Enting, R. H., Bienfait, H. P., Robe, P., Baumert, B. G., Visser, O., & Dutch Society for Neuro-Oncology (LWNO). (2014). Changing incidence and improved survival of gliomas. *European Journal of Cancer*, *50*, 2309–2318. https://doi.org/10.1016/j.ejca.2014.05.019

Hsieh, C. L., Koike, M., Spusta, S. C., Niemi, E. C., Yenari, M., Nakamura, M. C., & Seaman, W. E. (2009). A role for TREM2 ligands in the phagocytosis of apoptotic neuronal cells by microglia. *Journal of Neurochemistry*, *109*, 1144–1156.

Hu, F., Dzaye, O. D., Hahn, A., Yu, Y., Scavetta, R. J., Dittmar, G., Kaczmarek, A. K., Dunning, K. R., Ricciardelli, C., Rinnenthal, J. L., Heppner, F. L., Lehnardt, S., Synowitz, M., Wolf, S. A., & Kettenmann, H. (2015). Glioma-derived versican promotes tumor expansion via glioma-associated microglial/macrophages toll-like receptor 2 signaling. *Neuro-Oncology*, *17*, 200–210.

Huang, Y., Zhang, Q., Lubas, M., Yuan, Y., Yalcin, F., Efe, I., Xia, P., Motta, E., Buonfiglioli, A., Lehnardt, S., Dzaye, O., Flueh, C., Synowitz, M., Hu, F., & Kettenmann, H. (2020). Synergistic toll-like receptor 3/9 signaling affects properties and impairs glioma-promoting activity of microglia. *The Journal of Neuroscience*, *40*, 6428–6443.

Jackson, C. M., Choi, J., & Lim, M. (2019). Mechanisms of immunotherapy resistance: Lessons from glioblastoma. *Nature Immunology*, *20*, 1100–1109. https://doi.org/10.1038/s41590-019-0433-y

Katzenelenbogen, Y., Sheban, F., Yalin, A., Yofe, I., Svetlichnyy, D., Jaitin, D. A., Bornstein, C., Moshe, A., Keren-Shaul, H., Cohen, M., Wang, S.-Y., Li, B., David, E., Salame, T.-M., Weiner, A., & Amit, I. (2020). Coupled scRNA-Seq and intracellular protein activity reveal an immunosuppressive role of TREM2 in cancer. *Cell*, *182*, 872–885.e19. https://doi.org/10.1016/j.cell.2020.06.032

Kilian, M., Sheinin, R., Tan, C. L., Friedrich, M., Krämer, C., Kaminitz, A., Sanghvi, K., Lindner, K., Chih, Y.-C., Cichon, F., Richter, B., Jung, S., Jähne, K., Ratliff, M., Prins, R. M., Etminan, N., von Deimling, A., Wick, W., Madi, A., ... Platten, M. (2023). MHC class II-restricted antigen presentation is required to prevent dysfunction of cytotoxic T cells by blood-borne myeloids in brain tumors. *Cancer Cell*, *41*, 235–251.e9.

Kleinberger, G., Brendel, M., Mracsko, E., Wefers, B., Groeneweg, L., Xiang, X., Focke, C., Deußing, M., Suárez-Calvet, M., Mazaheri, F., Parhizkar, S., Pettkus, N., Wurst, W., Feederle, R., Bartenstein, P., Mueggler, T., Arzberger, T., Knuesel, I., Rominger, A., & Haass, C. (2017). The FTD-like syndrome causing TREM2 T66M mutation impairs microglia function, brain perfusion, and glucose metabolism. *EMBO Journal*, *36*, 1837–1853. https://doi.org/10.15252/embj.201796516

Kleinberger, G., Yamanishi, Y., Suárez-Calvet, M., Czirr, E., Lohmann, E., Cuyvers, E., Struyfs, H., Pettkus, N., Wenninger-Weinzierl, A., Mazaheri, F., Tahirovic, S., Lleó, A., Alcolea, D., Fortea, J., Willem, M., Lammich, S., Molinuevo, J. L., Sánchez-Valle, R., Antonell, A., ... Haass, C. (2014). TREM2 mutations implicated in neurodegeneration impair cell surface transport and phagocytosis. *Science Translational Medicine*, *6*, 243ra86.

Klemm, F., Maas, R. R., Bowman, R. L., Kornete, M., Soukup, K., Nassiri, S., Brouland, J. P., Iacobuzio-Donahue, C. A., Brennan, C., Tabar, V., Gutin, P. H., Daniel, R. T., Hegi, M. E., & Joyce, J. A. (2020). Interrogation of the microenvironmental landscape in brain tumors reveals disease-specific alterations of immune cells. *Cell*, *181*, 1643–1660.e17. https://doi.org/10.1016/j.cell.2020.05.007

Lewcock, J. W., Schlepckow, K., Di Paolo, G., Tahirovic, S., Monroe, K. M., & Haass, C. (2020). Emerging microglia biology defines novel therapeutic approaches for Alzheimer's disease. *Neuron*, *108*, 801–821. https://doi.org/10.1016/j.neuron.2020.09.029

Lim, E.-J., Kang, J.-H., Kim, Y.-J., Kim, S., & Lee, S.-J. (2022). ICAM-1 promotes cancer progression by regulating SRC activity as an adapter protein in colorectal cancer. *Cell Death & Disease*, *13*, 417.

Lim, M., Xia, Y., Bettegowda, C., & Weller, M. (2018). Current state of immunotherapy for glioblastoma. *Nature Reviews Clinical Oncology*, *15*, 422–442. https://doi.org/10.1038/s41571-018-0003-5

Liu, Y.-Y., Yao, R.-Q., Long, L.-Y., Liu, Y.-X., Tao, B.-Y., Liu, H.-Y., Liu, J.-L., Li, Z., Chen, L., & Yao, Y.-M. (2022). Worldwide productivity and research trend of publications concerning glioma-associated macrophage/microglia: A bibliometric study. *Frontiers in Neurology*, *13*, 1047162.

Machein, M. R., & Plate, K. H. (2000). VEGF in brain tumors. *Journal of Neuro-Oncology*, *50*, 109–120.

Massey, S. C., Whitmire, P., Doyle, T. E., Ippolito, J. E., Mrugala, M. M., Hu, L. S., Canoll, P., Anderson, A. R. A., Wilson, M. A., Fitzpatrick, S. M., McCarthy, M. M., Rubin, J. B., & Swanson, K. R. (2021). Sex differences in health and disease: A review of biological sex differences relevant to cancer with a spotlight on glioma. *Cancer Letters*, *498*, 178–187. https://doi.org/10.1016/j.canlet.2020.07.030

Mazaheri, F., Snaidero, N., Kleinberger, G., Madore, C., Daria, A., Werner, G., Krasemann, S., Capell, A., Trümbach, D., Wurst, W., Brunner, B., Bultmann, S., Tahirovic, S., Kerschensteiner, M., Misgeld, T., Butovsky, O., & Haass, C. (2017). TREM2 deficiency impairs chemotaxis and microglial responses to neuronal injury. *EMBO Reports*, *18*, 1186–1198. https://doi.org/10.15252/embr.201743922

Molgora, M., Esaulova, E., Vermi, W., Hou, J., Chen, Y., Luo, J., Brioschi, S., Bugatti, M., Omodei, A. S., Ricci, B., Fronick, C., Panda, S. K., Takeuchi, Y., Gubin, M. M., Faccio, R., Cella, M., Gilfillan, S., Unanue, E. R., Artyomov, M. N., ... Colonna, M. (2020). TREM2 modulation remodels the tumor myeloid landscape enhancing anti-PD-1 immunotherapy. *Cell*, *182*, 886–900.e17. https://doi.org/10.1016/j.cell.2020.07.013

Osterberg, N., Ferrara, N., Vacher, J., Gaedicke, S., Niedermann, G., Weyerbrock, A., Doostkam, S., Schaefer, H.-E., Plate, K. H., & Machein, M. R. (2016). Decrease of VEGF-A in myeloid cells attenuates glioma progression and prolongs survival in an experimental glioma model. *Neuro-Oncology*, *18*, 939–949.

Ostrom, Q. T., Gittleman, H., Truitt, G., Boscia, A., Kruchko, C., & Barnholtz-Sloan, J. S. (2018). CBTRUS statistical report: Primary brain and other central nervous system tumors diagnosed in the United States in 2011–2015. *Neuro-Oncology*, *20*, iv1–iv86.

Ostrom, Q. T., Rubin, J. B., Lathia, J. D., Berens, M. E., & Barnholtz-Sloan, J. S. (2018). Females have the survival advantage in glioblastoma. *Neuro-Oncology*, *20*, 576–577.

Pan, Y., Smithson, L. J., Ma, Y., Hambardzumyan, D., & Gutmann, D. H. (2017). Ccl5 establishes an autocrine high-grade glioma growth regulatory circuit critical for mesenchymal glioblastoma survival. *Oncotarget*, *8*, 32977–32989.

Roesch, S., Rapp, C., Dettling, S., & Herold-Mende, C. (2018). When immune cells turn bad-tumor-associated microglia/macrophages in glioma. *International Journal of Molecular Sciences*, *19*, 436.

Schaff, L. R., & Mellinghoff, I. K. (2023). Glioblastoma and other primary brain malignancies in adults: A review. *JAMA*, *329*, 574–587.

Schlepckow, K., Monroe, K. M., Kleinberger, G., Cantuti-Castelvetri, L., Parhizkar, S., Xia, D., Willem, M., Werner, G., Pettkus, N., Brunner, B., Sülzen, A., Nuscher, B., Hampel, H., Xiang, X., Feederle, R., Tahirovic, S., Park, J. I., Prorok, R., Mahon, C., ... Haass, C. (2020). Enhancing protective microglial activities with a dual function TREM2 antibody to the stalk region. *EMBO Molecular Medicine*, *12*, e11227. https://doi.org/10.15252/emmm.201911227

Shi, Y., Huang, X., Chen, G., Wang, Y., Liu, Y., Xu, W., Tang, S., Guleng, B., Liu, J., & Ren, J. (2019). miR-632 promotes gastric cancer progression by accelerating angiogenesis in a TFF1-dependent manner. *BMC Cancer*, *19*, 14.

Silva, R., D'Amico, G., Hodivala-Dilke, K. M., & Reynolds, L. E. (2008). Integrins: The keys to unlocking angiogenesis. *Arteriosclerosis, Thrombosis, and Vascular Biology*, *28*, 1703–1713.

Suffee, N., Richard, B., Hlawaty, H., Oudar, O., Charnaux, N., & Sutton, A. (2011). Angiogenic properties of the chemokine RANTES/CCL5. *Biochemical Society Transactions*, *39*, 1649–1653.

Sun, R., Han, R., McCornack, C., Khan, S., Tabor, G. T., Chen, Y., Hou, J., Jiang, H., Schoch, K. M., Mao, D. D., Cleary, R., Yang, A., Liu, Q., Luo, J., Petti, A., Miller, T. M., Ulrich, J. D., Holtzman, D. M., & Kim, A. H. (2023). TREM2 inhibition triggers antitumor cell activity of myeloid cells in glioblastoma. *Science Advances*, *9*, eade3559.

Turkowski, K., Brandenburg, S., Mueller, A., Kremenetskaia, I., Bungert, A. D., Blank, A., Felsenstein, M., & Vajkoczy, P. (2018). VEGF as a modulator of the innate immune response in glioblastoma. *Glia*, *66*, 161–174.

Turnbull, I. R., Gilfillan, S., Cella, M., Aoshi, T., Miller, M., Piccio, L., Hernandez, M., & Colonna, M. (2006). Cutting edge: TREM-2 attenuates macrophage activation. *The Journal of Immunology*, *177*, 3520–3524.

VanRyzin, J. W., Marquardt, A. E., Pickett, L. A., & McCarthy, M. M. (2020). Microglia and sexual differentiation of the developing brain: A focus on extrinsic factors. *Glia*, *68*, 1100–1113.

VanRyzin, J. W., Pickett, L. A., & McCarthy, M. M. (2018). Microglia: Driving critical periods and sexual differentiation of the brain. *Developmental Neurobiology*, *78*, 580–592.

Wang, S., Mustafa, M., Yuede, C. M., Salazar, S. V., Kong, P., Long, H., Ward, M., Siddiqui, O., Paul, R., Gilfillan, S., Ibrahim, A., Rhinn, H., Tassi, I., Rosenthal, A., Schwabe, T., & Colonna, M. (2020). Anti-human TREM2 induces microglia proliferation and reduces pathology in an Alzheimer's disease model. *Journal of Experimental Medicine*, *217*, e20200785.

Wang, S.-W., Liu, S.-C., Sun, H.-L., Huang, T.-Y., Chan, C.-H., Yang, C.-Y., Yeh, H.-I., Huang, Y.-L., Chou, W.-Y., Lin, Y.-M., & Tang, C.-H. (2015). CCL5/CCR5 axis induces vascular endothelial growth factor-mediated tumor angiogenesis in human osteosarcoma microenvironment. *Carcinogenesis*, *36*, 104–114.

Wu, W., Klockow, J. L., Zhang, M., Lafortune, F., Chang, E., Jin, L., Wu, Y., & Daldrup-Link, H. E. (2021). Glioblastoma multiforme (GBM): An overview of current therapies and mechanisms of resistance. *Pharmacological Research*, *171*, 105780. https://doi.org/10.1016/j.phrs.2021.105780

Xiang, X., Piers, T. M., Wefers, B., Zhu, K., Mallach, A., Brunner, B., Kleinberger, G., Song, W., Colonna, M., Herms, J., Wurst, W., Pocock, J. M., & Haass, C. (2018). The Trem2 R47H Alzheimer's risk variant impairs splicing and reduces Trem2 mRNA and protein in mice but not in humans. *Molecular Neurodegeneration*, *13*, 49.

Xiang, X., Werner, G., Bohrmann, B., Liesz, A., Mazaheri, F., Capell, A., Feederle, R., Knuesel, I., Kleinberger, G., & Haass, C. (2016). TREM2 deficiency reduces the efficacy of immunotherapeutic amyloid clearance. *EMBO Molecular Medicine*, *8*, 992–1004.

Xie, M., Liu, Y. U., Zhao, S., Zhang, L., Bosco, D. B., Pang, Y. P., Zhong, J., Sheth, U., Martens, Y. A., Zhao, N., Liu, C. C., Zhuang, Y., Wang, L., Dickson, D. W., Mattson, M. P., Bu, G., & Wu, L. J. (2022). TREM2 interacts with TDP-43 and mediates microglial neuroprotection against TDP-43-related neurodegeneration. *Nature Neuroscience*, *25*, 26–38.

Yang, W., Warrington, N. M., Taylor, S. J., Whitmire, P., Carrasco, E., Singleton, K. W., Wu, N., Lathia, J. D., Berens, M. E., Kim, A. H., Barnholtz-Sloan, J. S., Swanson, K. R., Luo, J., & Rubin, J. B. (2019). Sex differences in GBM revealed by analysis of patient imaging, transcriptome, and survival data. *Science Translational Medicine*, *11*, 1–15.

Yin, W., Ping, Y. F., Li, F., Lv, S. Q., Zhang, X. N., Li, X. G., Guo, Y., Liu, Q., Li, T. R., Yang, L. Q., Yang, K. D., Liu, Y. Q., Luo, C. H., Luo, T., Wang, W. Y., Mao, M., Luo, M., He, Z. C., Cao, M. F., ... Bian, X. W. (2022). A map of the spatial distribution and tumour associated macrophage states in glioblastoma and grade 4 IDH-mutant astrocytoma. *The Journal of Pathology*, *258*, 121–135.

Zhang, C., Wang, N., Tan, H.-Y., Guo, W., Chen, F., Zhong, Z., Man, K., Tsao, S. W., Lao, L., & Feng, Y. (2020). Direct inhibition of the TLR4/MyD88 pathway by geniposide suppresses HIF-1α-independent VEGF expression and angiogenesis in hepatocellular carcinoma. *British Journal of Pharmacology*, *177*, 3240–3257.

Zhang, J., Wang, H., Yuan, C., Wu, J., Xu, J., Chen, S., Zhang, C., & He, Y. (2022). ITGAL as a prognostic biomarker correlated with immune infiltrates in gastric cancer. *Frontiers in Cell and Developmental Biology*, *10*, 808212.

Zhang, W., Zhang, D., Cheng, Y., Liang, X., & Wang, J. (2022). Runx1 regulates Tff1 expression to expedite viability of retinal microvascular endothelial cells in mice with diabetic retinopathy. *Experimental Eye Research*, *217*, 108969. https://doi.org/10.1016/j.exer.2022.108969

Zhao, L., Wang, Y., Xue, Y., Lv, W., Zhang, Y., & He, S. (2015). Critical roles of chemokine receptor CCR5 in regulating glioblastoma proliferation and invasion. *Acta Biochimica et Biophysica Sinica*, *47*, 890–898.

Zhao, Z., Zhang, K.-N., Wang, Q., Li, G., Zeng, F., Zhang, Y., Wu, F., Chai, R., Wang, Z., Zhang, C., Zhang, W., Bao, Z., & Jiang, T. (2021). Chinese glioma genome atlas (CGGA): A comprehensive resource with functional genomic data from Chinese glioma patients. *Genomics Proteomics Bioinformatics*, *19*, 1–12. https://doi.org/10.1016/j.gpb.2020.10.005

SUPPORTING INFORMATION

Additional supporting information can be found online in the Supporting Information section at the end of this article.

How to cite this article: Chen, X., Zhao, Y., Huang, Y., Zhu, K., Zeng, F., Zhao, J., Zhang, H., Zhu, X., Kettenmann, H., & Xiang, X. (2023). TREM2 promotes glioma progression and angiogenesis mediated by microglia/brain macrophages. *Glia*, *71*(11), 2679–2695. https://doi.org/10.1002/glia.24456